Thermoelectric transport in two-dimensional disordered systems

R. T. Syme and M. J. Kearney
GEC-Marconi Ltd., Hirst Research Centre, East Lane, Wembley, Middlesex, HA9 7PP, United Kingdom
(Received 16 March 1992)

We present evidence for the observation of localization and interaction corrections to the thermoelectric coefficient η relating current flow to applied temperature gradient, using the two-dimensional electron gas of a silicon-on-sapphire metal-oxide-semiconductor field-effect transistor as a test system. The present state of the theory of such corrections is discussed in detail, including effects such as phonon drag and phonon renormalization. The experimental apparatus which we use to measure η as a function of magnetic field is then described. In a perpendicular magnetic field we observe an increase in the magnitude of η which is explained in terms of suppression of quantum interference effects by the field: we find good agreement between experiment and theory. For a parallel magnetic field we are able to show that there is a nonzero interaction correction to η, and we put bounds on the size of this effect.

I. INTRODUCTION

Extensive investigations of the electrical conductivity σ of disordered solids have revealed a number of interesting effects, related to the suppression of localization on the one hand, and to the enhancement of electron-electron interactions on the other. Both may be studied more or less independently by exploiting the greater sensitivity of the localization mechanism to weak magnetic fields.[1] The agreement between theory and experiment in weakly disordered samples is, with few exceptions, generally satisfactory. This is not the situation regarding all other transport coefficients, however, especially those which involve response to an applied temperature gradient.

Of the thermal transport coefficients most commonly studied in disordered solids, the thermopower S is probably the easiest to measure. Almost all this work has concentrated on observing changes in S with temperature; very little attention seems to have been devoted to studying changes of S in a weak magnetic field, which is surprising given the wealth of information obtained from magnetoresistance measurements. Comparison between experiment and theory is complicated, however, by the fact that S cannot be calculated directly; rather it is a composite quantity of the electrical conductivity and a thermoelectric coefficient η which relates the current flowing in response to an applied temperature gradient (S is measured under conditions of zero current flow). The challenge therefore is to try to extract from measurements of S and σ the parameter η about which less is known in disordered systems.

In a recent paper,[2] evidence was presented for localization corrections to η which are quite distinct from those to σ. The system studied there was the two-dimensional electron gas (2D EG) in the inversion layer of a silicon-on-sapphire (SOS) metal-oxide-semiconductor field-effect transistor (MOSFET). In the present paper these results are expanded upon by examining the different behaviors observed in magnetic fields applied both parallel and perpendicular to the inversion layer, elucidating the interplay between localization effects and interaction effects. Attention is given to discussing some of the more unusual features of thermoelectric transport in disordered solids, such as phonon renormalization[3] and phonon drag.[4] In electrical conductivity measurements the phonons are basically irrelevant, which is one way in which the present experiments are of fundamental interest.

The paper is organized as follows. In Sec. II the theory (as it is currently understood) of thermoelectric transport in disordered systems is reviewed. In Sec. III, details of the experimental methods used are discussed. Detailed results and analysis for the silicon-on-sapphire MOSFET system are presented in Sec. IV. Finally, in Sec. V, conclusions are drawn and a number of the outstanding issues remaining to be resolved are highlighted.

II. THERMOELECTRIC TRANSPORT: THEORETICAL CONSIDERATIONS

A. Classical magnetotransport

The basic geometry of the two-dimensional electron system is depicted in Fig. 1. In response to an electromotive force $\mathbf{E}$ and a temperature gradient ∇T we write to linear order

$$\mathbf{J}=\underline{L}^{11}\mathbf{E}-(\underline{L}^{12}/T)\nabla T\ , \tag{2.1}$$

$$\mathbf{J}^q=\underline{L}^{21}\mathbf{E}-(\underline{L}^{22}/T)\nabla T\ , \tag{2.2}$$

where $\mathbf{J}$ and $\mathbf{J}^q$ are the electric current and heat current, respectively, and $\mathbf{E}=\mathbf{F}-(1/q)\nabla\mu$, where $\mathbf{F}$ is the applied electric field and μ is the chemical potential. The charge on the carriers is denoted by q throughout *and is negative for electrons.* The $\underline{L}^{ij}$ are tensors and are defined more formally in the next section. They are the natural quantities to calculate. Only $\underline{L}^{11}$ has a standard interpretation, being the electrical conductivity tensor $\underline{\sigma}$, and often the others are written using a different notation. For example, in Ref. 2, Eq. (2.1) was written as

$$\mathbf{J}=\underline{\sigma}\mathbf{E}-\underline{\eta}\nabla T \ . \tag{2.3}$$

In the present discussion we will adhere to this latter form, so as to maintain continuity with the earlier paper.

In the Drude model of the electrical conductivity, the various components of the conductivity tensor under steady-state conditions are given by (assuming an isotropic mass m^*)

$$\sigma_{xx}=\sigma_{yy}=\frac{\sigma_0}{1+\omega_c^2\tau^2} \ , \tag{2.4}$$

$$\sigma_{xy}=-\sigma_{yx}=\sigma_0\left[\frac{\omega_c\tau}{1+\omega_c^2\tau^2}\right] \ , \tag{2.5}$$

$$\sigma_0=\frac{nq^2\tau}{m^*} \ , \tag{2.6}$$

where $\omega_c=qB_z/m^*$ (the cyclotron frequency is $|\omega_c|$), n is the electron concentration, τ is the relaxation time, B_z is the z component of the magnetic field, and σ_0 is the diagonal conductivity in the absence of a field. All the components of $\underline{\sigma}$ have a contribution from classical magneto-orbital effects. Quantum corrections calculated for σ_{xx} in weak fields[1] ($\omega_c\tau\ll 1$) may be thought of as arising from corrections to the transport time τ. To leading order, it is not unreasonable to assume that this interpretation survives to somewhat larger fields and that Eqs. (2.4)–(2.6) can continue to be used with the quantum corrections confined to altering τ in both the numerators and denominators. A similar set of equations may be written down for the components of the thermoelectric tensor η with σ_0 replaced with η_0 (to be defined in the next section). The consequences of this become clear when one considers the quantities that are actually measured as opposed to those that are calculated.

Instead of applying an electromotive force and measuring the resulting current, it is more convenient experimentally to apply an electric current and measure the resulting electromotive force. We write

$$\mathbf{E}=\underline{\rho}\mathbf{J}+\underline{S}\nabla T \ , \tag{2.7a}$$

$$\mathbf{J}^q=\underline{\pi}\mathbf{J}-\underline{\kappa}\nabla T \ , \tag{2.7b}$$

where the transport coefficients are known as the resistivity $\underline{\rho}$, the thermopower $\underline{S}$, the Peltier coefficient $\underline{\pi}$, and the thermal conductivity $\underline{\kappa}$, respectively. In this paper we will be concerned with measurements of the ρ_{xx} component of the resistivity tensor and the S_{xx} component of the thermopower tensor. During such measurements, the current in the y direction is strictly zero (although the transverse electric field E_y is nonzero in a magnetic field) and it is assumed that the temperature gradient in the y direction is also zero (see Sec. III A). Relating ρ_{xx} to calculated quantities we find that

$$\rho_{xx}=\frac{\sigma_{yy}}{\sigma_{xx}\sigma_{yy}-\sigma_{xy}\sigma_{yx}}=\frac{1}{\sigma_0} \ , \tag{2.8}$$

i.e., within the Drude model there is no magnetoresistance (a well-known feature). Less well known is the fact that a similar result holds for S_{xx},

$$S_{xx}=\frac{\sigma_{yy}\eta_{xx}-\sigma_{xy}\eta_{yx}}{\sigma_{xx}\sigma_{yy}-\sigma_{xy}\sigma_{yx}}=\frac{\eta_0}{\sigma_0} \ , \tag{2.9}$$

which is also independent (at this level of calculation) of magnetic field. The interpretation here is that since S_{xx} is measured under conditions of zero net current flow (or as near this as can be attained), the magnetic field cannot have an effect (classically) as it contributes through a term $\mathbf{v}\times\mathbf{B}$ whose average value (over all carriers) is zero. One can therefore equate the experimentally measured quantities with theoretical quantities such as σ ($=1/\rho_{xx}$) and η ($=S_{xx}/\rho_{xx}$) which are calculated under the assumption that there are no classical magnetotransport effects. This is a stronger statement than the one usually made that classical effects can be ignored when $\omega_c\tau\ll 1$. The above conclusions are not affected by having an anisotropic effective mass such as is found in the silicon-on-sapphire system, for example, as may easily be demonstrated.

B. Quantum interference and interaction effects (for $B=0$)

In the absence of a magnetic field and for an isotropic system we can write $\underline{L}^{ij}=L^{ij}\underline{I}$, where $\underline{I}$ is the identity matrix and L^{ij} is a scalar quantity. The transport coefficients L^{ij} may be calculated formally in a number of ways; the most conventional method is via the Kubo formula.[5] Calculations of both quantum interference (localization) and interaction corrections to the electrical conductivity of disordered systems (based on a diagrammatic expansion of the Kubo formula) have been very successful and are well documented elsewhere.[1]

Calculations of the thermal transport coefficients (such as η) on the other hand are highly nontrivial.[5] Exact results (where they are available) are therefore very useful. One, which is relevant to the present discussion, was derived by Chester and Thellung.[6] Their theorem assumes that the electrons are noninteracting and that the scattering is elastic, but is otherwise completely general and, in particular, makes no assumption about the strength of the disorder. Under these conditions the transport coefficients are related to one another as follows:[7]

$$L^{ij}=\int G(\varepsilon)\left[\frac{\varepsilon-\mu}{q}\right]^{i+j-2}\left[-\frac{\partial f}{\partial\varepsilon}\right]d\varepsilon \ , \tag{2.10}$$

where $f(\varepsilon-\mu)$ is the Fermi-Dirac distribution function, μ is the chemical potential, and all the information about the disorder is contained in the function $G(\varepsilon)$. Equation (2.10) can be made the basis for a number of important predictions[7] because the function $G(\varepsilon)$ is common to all the L^{ij}. The connection between σ and $G(\varepsilon)$ is clear: $G(\varepsilon)$ may be interpreted as an energy-dependent conductivity. At low temperatures, where $G(\varepsilon)$ is slowly varying on the scale of k_BT, we can expand to show that the diffusion thermopower S_d is given by

$$S_d=\frac{\eta}{\sigma}=\frac{\pi^2k_B^2}{3q}T\left[\frac{d\ln G(\varepsilon)}{d\varepsilon}\right]_{\varepsilon=\mu} \ , \tag{2.11}$$

which is the well-known Mott formula.[8] Also, the

thermal conductivity κ is given to an excellent approximation by

$$\kappa \approx L^{22}/T = \frac{\pi^2 k_B^2}{3q^2} TG(\mu) . \tag{2.12}$$

A consequence of the last result is that the Wiedemann-Franz law,

$$\lim_{T\to 0}\left[\frac{\kappa}{\sigma T}\right] = \frac{\pi^2 k_B^2}{3q^2} \approx 2.44\times 10^{-8}\ \mathrm{W\,\Omega\,K^{-2}} , \tag{2.13}$$

is valid for arbitrary strength of disorder,[6,7] a striking conclusion for which there is now a growing body of experimental evidence.[9]

One needs to be very careful in treating all the different energy-dependent contributions when carrying out calculations to obtain the correct answer. For example, to lowest order in the disorder it is common to write [cf. Eq. (2.6)]

$$G_0(\varepsilon) = \frac{n(\varepsilon) q^2 \tau(\varepsilon)}{m^*} \sim \varepsilon^{d/2+p} , \tag{2.14}$$

where d is the system dimensionality and p is the exponent of the relaxation rate, i.e., $1/\tau(\varepsilon)\sim\varepsilon^{-p}$. We therefore derive

$$\eta_0 \approx \frac{\pi^2 k_B^2}{3q} T \frac{(d/2+p)}{\mu} \sigma_0 , \tag{2.15}$$

with $S_d = \eta_0/\sigma_0$. The magnitude of the diffusion thermopower is clearly dependent on the exponent p which is nonuniversal. Indeed, it is even possible for S_d to change sign (from its "conventional" negative to positive) in a system where the relaxation rate increases sufficiently ($p < -d/2$) as the energy increases.[10]

Equation (2.13) implies that there are no weak-localization corrections to the Wiedemann-Franz law, i.e., the corrections to κ exactly cancel those of σ.[11] The first calculation of weak-localization corrections to η suggested a similar behavior whereby the correction to η also canceled the correction to σ, leaving the diffusion thermopower unaltered.[12] This conclusion is now believed to be erroneous and subsequent calculations have revealed that there are corrections to the diffusion thermopower due to localization.[13] Such corrections to S_d have been observed experimentally near a metal-insulator transition.[14] Their form may be derived in a satisfying and intuitive way from the Chester-Thellung theorem.[7] Thus, for example, if we write

$$\sigma(\varepsilon) = \sigma_0(\varepsilon) + \delta\sigma^{\mathrm{loc}}(\varepsilon, T) \tag{2.16}$$

and replace $G(\varepsilon)$ in Eq. (2.10) with $\sigma(\varepsilon)$, the correct result is obtained,

$$\delta\eta^{\mathrm{loc}}(\mu, T) = \frac{\pi^2 k_B^2}{3q} T \left[\frac{d}{d\varepsilon}\delta\sigma^{\mathrm{loc}}(\varepsilon, T)\right]_{\varepsilon=\mu} , \tag{2.17}$$

since Eq. (2.10) holds for arbitrary disorder and is therefore valid in the weak-localization regime (defined by $k_F l \gg 1$, where k_F is the Fermi wave vector and l is the mean free path). The implied inelastic scattering required for phase breaking is not expected to violate the condition under which the Chester-Thellung result is derived (i.e., predominantly elastic scattering). Only when the inelastic scattering rate is large would we expect the results to significantly deviate. The correction has a linear temperature dependence (the same as that of η_0) with $|\delta\eta^{\mathrm{loc}}(T)/\eta_0(T)|$ of order $(k_F l)^{-1}$, and experimentally it is not possible to distinguish the two on the basis of temperature measurements alone. The *thermopower* itself has a $\ln T$ correction, but one which arises from the conductivity correction only.

The same approach cannot be applied to the case of interaction corrections, where the assumptions under which Eq. (2.10) was derived are fundamentally violated. Here one must resort to perturbation theory to calculate the interaction correction $\delta\eta^{\mathrm{int}}$ directly. The original calculation, due to Ting, Houghton, and Senna,[12] concluded that in two dimensions $\delta\eta^{\mathrm{int}} \sim T\ln T$, although their calculation has been questioned.[15,16] Hsu, Kapitulnik, and Reizer[15] carried out the calculation using the Keldysh diagram technique and concluded that there is no logarithmic temperature correction to η due to interaction effects. However, Fabrizio, Castellani, and Strinati[16] found that a $T\ln T$ term should be present, but with a different prefactor from that predicted by Ting, Houghton, and Senna.[12] The situation regarding the theoretical status of interaction corrections to η (and hence the thermopower) therefore remains somewhat confused. Nor do we expect the controversy to be resolved experimentally on the basis of temperature measurements alone. For instance, we can write the diffusion thermopower as

$$S_d(T,B) = \frac{\eta_0(T) + \delta\eta^{\mathrm{loc}}(T,B) + \delta\eta^{\mathrm{int}}(T)}{\sigma_0 + \delta\sigma^{\mathrm{loc}}(T,B) + \delta\sigma^{\mathrm{int}}(T)} , \tag{2.18}$$

where, in two dimensions, both $\delta\sigma^{\mathrm{loc}}$ and $\delta\sigma^{\mathrm{int}}$ are proportional to $\ln T$. Attributing a $T\ln T$ dependence to $\delta\eta^{\mathrm{int}}(T)$ from measurements of the temperature dependence of $S_d(T)$ [or $S_d(T)/T$] is clearly impractical. This is why magnetic-field measurements are expected to be such a powerful tool in beginning to unravel all the different effects (see Sec. II D). In Eq. (2.18), those contributions which are sensitive to weak magnetic fields ($g\mu_B B \ll k_B T$) are indicated, where g is the g factor and μ_B is the Bohr magneton.

C. The role of phonons ($B = 0$)

Whereas phonons are basically irrelevant as far as the low-temperature electrical conductivity is concerned, they play an important role in thermoelectric transport. Two processes are of interest, namely, phonon drag and phonon renormalization, and each is discussed below.

Unlike the electron-electron vertex, there is no enhancement [to order $(k_F l)^{-1}$] of the long-wavelength electron-phonon vertex due to the disorder.[17,18] As a result, it is believed that there are no significant phonon corrections to the electrical conductivity at low temperatures, although there are expected to be some contributions at higher temperatures arising from electron-phonon-impurity processes.[19,20] The details remain un-

clear, however. The situation regarding the thermopower, even at the most fundamental level, is more controversial still. The basic issue concerns whether or not η_0 (defined in the preceding section) should be replaced by $\eta_0(1+\lambda)$, where λ is a renormalization factor due to the phonons.

Many different answers have been obtained for λ depending upon the assumptions made.[21] The most recent calculation of which we are aware carries out the analysis using the Keldysh diagram technique, which calculates η directly and so avoids the problems inherent in choosing the correct heat current operator.[22] The conclusion is that (in 3D) $\lambda=0$ if the impurity scattering is treated within the Born approximation, but is nonzero when the scattering is treated beyond the Born approximation. There is some experimental evidence that a nonzero value of λ can be observed in bulk disordered systems.[3,23] No calculations seem to be available for two-dimensional systems, however, or for what happens when the impurity interaction is treated beyond order $(k_F l)^{-1}$. We cannot say unequivocally, therefore, whether or not there should be a phonon renormalization enhancement to $\delta\eta^{\rm loc}$ [which is calculated to higher order in $(k_F l)^{-1}$], although it seems reasonable that if η_0 is renormalized, then so is $\delta\eta^{\rm loc}$.

This suggestion is strengthened by the following argument. In the limit of weak phonon scattering, or when the phonon scattering is treated within an adiabatic (elastic) approximation, the Chester-Thellung result [Eq. (2.10)] should be recovered. Jonson and Mahan[24] have shown that Eq. (2.10) actually holds to somewhat higher order, the only modification being the addition of a correction term which they estimate to be small. There are two consequences of this. Firstly, any phonon renormalization of η is due to phonon contributions to the electrical conductivity, which may appear small in the context of conductivity measurements, but whose energy derivatives are clearly crucial. Secondly, it strengthens the notion that the localization corrections to η are renormalized in a similar way to that of η_0, irrespective of system dimensionality.

In the presence of an applied temperature gradient there is a net flux of phonons in the direction of $-\nabla T$. The nonequilibrium nature of the phonons influences the electron transport and produces a contribution to η referred to as the phonon-drag component η_g. Often the phonon-drag contribution (characterized by a T^3 temperature dependence[4,25]) is significantly larger in magnitude than the diffusion contribution discussed in Sec. II B, although in very disordered samples where the phonon mean free path is severely limited it can often be ignored. It is usually assumed that the two contributions are additive, i.e., $\eta=\eta_d+\eta_g$. A detailed discussion of phonon drag in two-dimensional systems may be found in Refs. 26 and 27.

It is not expected that the nonequilibrium nature of the phonon distribution will affect any of the preceding discussion about η_d. We do need to know, on the other hand, if there is a localization correction to η_g. Quantum interference results in a modification of the electron diffusion constant[1] which might be expected to modify the electron-phonon interaction and hence η_g. We have seen, however, that the electron-phonon vertex is much less sensitive to the diffusive nature of electron motion than, say, the electron-electron vertex. It seems plausible then that the corrections to η_g owing to a change in the electron diffusion constant should be negligible, and hence that there is essentially no localization correction ($\delta\eta_g^{\rm loc}\sim 0$), although we have not proved this to be the case. A direct calculation would therefore be of some interest.

D. Quantum interference in the presence of a magnetic field

The localization correction for a two-dimensional system in the absence of the spin-orbit scattering is given by[1]

$$\delta\sigma^{\rm loc}(T,B_\perp)=\frac{g_v\alpha q^2}{2\pi^2\hbar}\left[\Psi\left\{\frac{1}{2}+\frac{\hbar}{4|q|B_\perp L_\phi^2}\right\}-\Psi\left\{\frac{1}{2}+\frac{\hbar}{4|q|B_\perp l^2}\right\}\right], \tag{2.19}$$

where g_v is a valley degeneracy factor, L_ϕ is the phase coherence length, Ψ is the digamma function, and $B_\perp$ is the component of the magnetic field perpendicular to the two-dimensional electron gas. The parameter α relates to intervalley scattering and is further discussed in Sec. IV B. In what follows, we will be interested primarily in the change of σ and η with magnetic field (applied both perpendicular and parallel to the 2D EG) for a fixed temperature. It is therefore convenient to introduce a new notation and define the quantities $\Delta\sigma(B)$ and $\Delta\eta(B)$ by $\Delta\sigma(B)\equiv\sigma(B)-\sigma(0)$ and $\Delta\eta(B)\equiv\eta(B)-\eta(0)$, respectively.

The destruction of quantum interference by a magnetic field implied by Eq. (2.19) leads to a positive magnetoconductance. Since the effect is orbital in origin, no change in conductivity is expected for a field applied parallel to the 2D EG, as long as the field remains weak. Likewise, the dominant interaction contributions (such as the Zeeman spin-splitting term) are also approximately independent of magnetic field for weak fields.[1] At larger fields the Zeeman term leads to a negative magnetoconductance, and one which is isotropic in terms of field orientation. The different behaviors allow the two contributions to be distinguished from one another, and typical examples for the Si-on-sapphire system will be presented in Sec. IV.

As far as η is concerned, Eq. (2.17) is expected to hold for weak fields. Including a possible phonon renormalization term we therefore have

$$\delta\eta^{\rm loc}(B,\mu,T)=\frac{\pi^2k_B^2}{3q}T(1+\lambda)\left[\frac{d}{d\varepsilon}\delta\sigma^{\rm loc}(B,\varepsilon,T)\right]_{\varepsilon=\mu}. \tag{2.20}$$

This result follows from the fact that the Chester-Thellung result can be shown to hold in a magnetic field,[8]

notwithstanding the problems of edge effects[28,29] which are negligible in the weak fields of interest. Under the assumption that interaction effects (based on particle-hole processes) are essentially independent of (weak) magnetic field (and here we make the additional assumption that the same holds for $\delta\eta^{\rm int}$ as $\delta\sigma^{\rm int}$, although no calculations have been carried out), Eq. (2.20) also holds for the quantity $\Delta\eta(B)$, with $\Delta\sigma(B)$ replacing $\delta\sigma^{\rm loc}$. The diffusion thermopower is therefore field dependent through those terms indicated in Eq. (2.18) (for weak fields). We assume that $\delta\eta_g^{\rm loc}\sim 0$ (even when a small field is present, as this only affects the diffusion constant) and this is the basis under which the results presented in the subsequent sections will be interpreted.

III. THERMOELECTRIC TRANSPORT: EXPERIMENTAL INVESTIGATIONS

As mentioned in Sec. I, the experimental difficulty associated with the measurement of thermoelectric effects in disordered 2D systems has meant that the primary focus of interest has been the electrical conductivity σ. However, a number of authors[30] have developed rather refined experimental techniques which have enabled accurate measurements of the thermopower to be made in such systems and these have yielded many interesting results. This section describes the problems encountered in measuring thermoelectric effects, the sort of experiments involved, and some of the techniques used to increase the accuracy and precision of the results.

A. What the experiments actually measure

Particular thermoelectric effects and their associated coefficients can be defined *locally* when certain special conditions apply to the currents, electric fields, and temperature gradients in a system.[31] If these conditions are experimentally realizable, then comparison with the corresponding *measurable* thermoelectric coefficient may be made. Note that we have made a distinction between the *locally defined* quantities and the *measurable* quantities. This is because the former are defined in terms of the components of the *gradients* of electrochemical potential and of temperature (and are therefore sometimes called differential thermoelectric coefficients), while the latter are defined in terms of the *difference* in the electrochemical potential or temperature *between two points.* The relation between the local and measurable coefficients can be obtained fairly easily provided that the following two conditions hold or at least hold to a good approximation.

(i) The applied temperature gradients and electric fields must be small enough that second-order effects are negligible. Here we confine ourselves to this linear approximation, but it must be emphasized that at very low temperatures, the temperature gradients may become quite large compared to the average temperature and that sometimes the measured quantities may not correspond to linear thermoelectric coefficients at all.[32]

(ii) The samples being measured must be homogeneous between the measurement points. One should be aware that the electrochemical potential drop can sometimes occur over only a small part of an electrically inhomogeneous 2D system in a semiconductor, even if the temperature drop is fairly uniform. Alternatively, there could be a voltage difference between two points at the same temperature if the temperature profile between them is not symmetric due to some inhomogeneity; this has been observed.[33]

Additionally, in a magnetic field one must be very clear as to whether the conditions are adiabatic ($J_y^q=0$) or isothermal ($\partial T/\partial y=0$). This is because the off-diagonal components of the tensors $\underline{L}^{ij}$ are nonzero when $B_z\neq 0$. Consider the setup in Fig. 1 with $\mathbf{J}=\mathbf{0}$ and with a magnetic field in the z direction. Equation (2.7a) shows that the longitudinal electromotive force E_x now contains a contribution from $\partial T/\partial y$ since S_{xy} can no longer be taken as equal to zero:

$$E_x = S_{xx}\partial T/\partial x + S_{xy}\partial T/\partial y \ . \tag{3.1}$$

Thus, although we still have $\Delta T=\Delta x\partial T/\partial x$ and $\Delta V_1=\Delta x E_x$ (assuming ΔT is small and the sample homogeneous), the *measured* longitudinal thermopower $\tilde{S}_1\equiv\Delta V_1/\Delta T=E_x/(\partial T/\partial x)$ is strictly no longer equal to S_{xx} unless the conditions are "isothermal," i.e., $\partial T/\partial y=0$. In most experiments on 2D systems in semiconductors the sample is not thermally isolated from its surroundings and heat can flow in the transverse direction through the metal wires used to contact the sample, thus making the isothermal condition more relevant to experiment. We assume this to be the case for our experiments. However, if adiabatic conditions were realized, then the measured transport coefficients would differ from those found under isothermal conditions. This could perhaps be the case if part of the 2D EG was heated directly, since it has been shown[34] that quite large electron temperature gradients can exist in a 2D EG, even though the lattice temperature is constant throughout the sample.

Although nearly all previous work on thermoelectric transport in 2D systems has focused on the thermopower $\underline{S}$, we are interested in obtaining the quantity η, relating current to applied temperature gradient. As discussed in Sec. II A, $\eta\equiv\underline{L}^{12}/T=\underline{\sigma}\,\underline{S}$. The quantity we extract is $\eta=S_{xx}/\rho_{xx}$, which differs from η_{xx} only by a semiclassical factor which is insignificant for our experiments. In

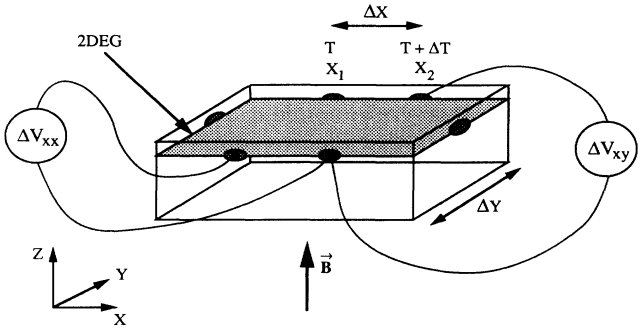

FIG. 1. Schematic diagram of our sample, showing directions of $\mathbf{B}$ and ∇T.

any case, as we have discussed, theoretical calculations tend to ignore semiclassical factors involving $\omega_c\tau$ and so generate this quantity η rather than η_{xx}.

B. Experimental techniques and samples

As compared with conventional electrical resistance and conductance measurements, the determination of thermoelectric transport coefficients requires considerably more refined experimental techniques. The longitudinal thermopower $\tilde{S}_1$ is the quantity most often obtained, and this requires the measurement of the temperature difference ΔT and voltage difference ΔV between two points in the presence of a small temperature gradient, as mentioned in the preceding section.

The samples used in this work were fabricated from (100) Si on $(\bar{1}012)$ sapphire wafers, with a Si thickness of 0.3 μm on average and a sapphire thickness of about 450 μm. The MOSFET's were fabricated using a standard metallic gate process, with an oxide thickness of 200 nm. The devices were 2000 μm long by 300 μm wide (lying along the [010] direction), with the side probes separated by 1300 μm [see Fig. 2(a)]. The mobilities were low (of the order of 500 $cm^2 V^{-1} s^{-1}$ at 4.2 K), because of the large amount of disorder present. At the end of the MOSFET's were resistors which were used as on-chip heaters in some experiments.

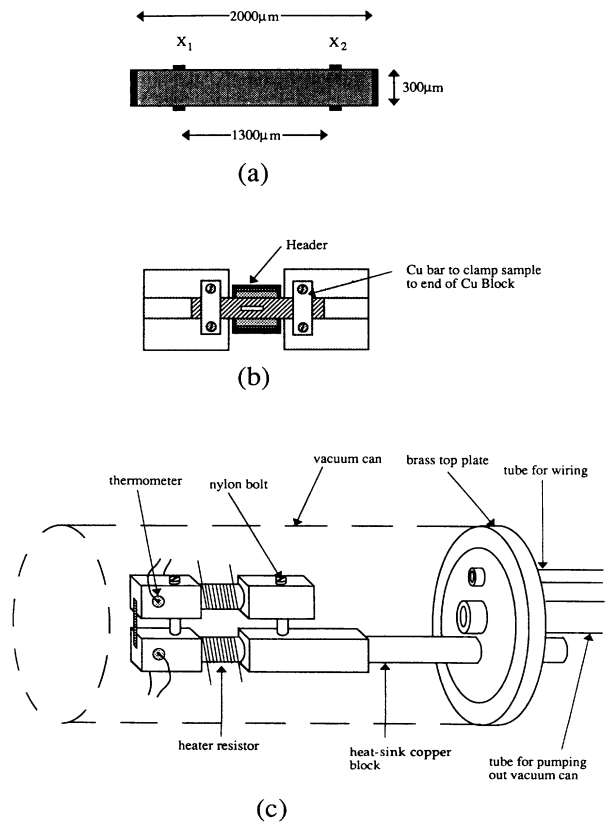

FIG. 2. (a) Geometry of MOSFET's used in this work. (b) Arrangement for clamping sample to end of insert. (c) Diagram of the insert used to measure the thermopower.

The sample holder consisted of two copper blocks [see Figs. 2(b) and 2(c)]. One of these acted as a heat sink to the ^{4}He bath and the other was attached to the first block with nylon bolts and low thermal conductivity spacers, leaving a gap of about 1 cm. Each block contained a calibrated resistance thermometer and a heater resistor, the latter in the form of a length of constantan wire wound around the block. The sample was clamped between the blocks, one end of the chip clamped onto the end of each block. Indium foil was found[35] to reduce the thermal resistance between sample and block. By applying currents to one or other of the heater resistors and changing the ^{4}He vapor pressure, the sample temperature and temperature gradient could be altered in a controlled way. The sample holder was enclosed in an evacuated can, so that the temperature gradient along the chip would not be "shorted-out" by the ^{4}He. Connections to the sample were made with either constantan wires (to reduce heat leaks) or, for measuring the thermopower, copper wires. The resistance thermometers were used to check that both copper blocks were in thermal equilibrium with the ^{4}He bath in the absence of a temperature gradient (the ^{4}He temperature was obtained by monitoring its vapor pressure).

Many of the techniques used for measuring ΔT and ΔV in 2D systems are similar to those used in 3D systems, but there are some added complications. Some measurements of the low-temperature thermopower of a 2D system were carried out by Zavaritskii and co-workers.[36] They used AuFe-Chromel thermocouples glued on to the sample to measure the temperature difference, with a superconducting quantum interference device (SQUID) as a null detector. A bridge arrangement, also using a SQUID, was used to measure the voltage difference. A similar setup was used by Obloh, von Klitzing, and Ploog,[37] but with a high-precision nanovoltmeter rather than a SQUID for measuring the voltages. Thermocouples are, however, rather fragile and cannot be used at high magnetic fields. In a series of elegant experiments, Fletcher *et al.*[38] used a pair of matched carbon resistance thermometers soldered to thin, flat pieces of copper wire which were then glued to the underside of their GaAs samples with epoxy. These could be checked at zero magnetic field with thermocouples, and calibrated for use at high magnetic fields as well.

However, thermal resistances can be a problem in thermopower measurements. As pointed out by Fletcher *et al.*,[39] there can be significant thermal resistances between the sample and the copper block which it is heatsunk to (they proposed that this could explain the anomalous results of Davidson *et al.*[40]). Even with our use of indium foil to reduce these thermal resistances, there was typically a 300 mK temperature difference between the blocks for a 50 mK difference between the side contacts of the MOSFET, about twice that expected for a linear temperature drop between the blocks. There are also liable to be thermal resistances between the sample and the thermocouples (or carbon resistance thermometers), leading to possible errors in the measurements of ΔT. To get round these difficulties, Gallagher *et al.*[41] proposed and demonstrated the method which we have used here.

Referring once again to Fig. 1, the conductance *across* the device (i.e., σ_{yy} multiplied by a geometrical factor) was measured at the two points x_1 and x_2, with no temperature gradient [using a conventional low-frequency (about 80 Hz) lock-in technique]. The temperature was then decreased by around 50–100 mK, and the conductances at x_1 and x_2 measured again. Finally, the temperature gradient was applied and the conductances measured again. Provided the temperature gradient is small enough, the conductances measured this time will fall between those measured previously, and the local temperature of the electron gas can be obtained by assuming a linear relationship between conductance and temperature over the small temperature range in question. This gives the temperature difference along the electron gas *directly*: there are no problems with thermal resistances between sample and thermometers. In practice, the differential mode on the lock-in amplifier was used to measure the difference between the conductances at x_1 and x_2 directly, thereby increasing the accuracy of the method. Notice that the form of the temperature dependence of the conductance is immaterial to this method. All that is required is that the temperature dependence is strong enough to give accurately measurable changes in the conductance, yet weak enough that it can be well represented by a linear approximation over the small temperature intervals used. In the disordered SOS MOSFET's which we used, the temperature dependence was logarithmic (due to weak localization[1]) over the measured temperature range 1.2–4.7 K, but for the small temperature interval used in finding ΔT, it could equally well be fitted by the linear approximation. Taking all the above factors into account, the uncertainty in a typical value of ΔT (30–50 mK) turned out to be about 1%.

The voltage difference ΔV was measured in two ways. For a constant temperature gradient, a Keithley 181 nanovoltmeter (with input impedance greater than 1 GΩ) was used: this could measure voltages down to 1 nV when steps were taken to improve the shielding and earthing arrangements. This gave the absolute values of thermopower with about a 1% uncertainty (notice that the uncertainties in S arising from geometrical considerations are small with these measurement techniques, because ΔV and ΔT are measured between the same side probes on the MOSFET). To allow measurements to be taken in a changing magnetic field, the temperature gradient was modulated at low frequencies (<5 Hz) by modulating the current supplied to the heater, and the thermoelectric voltage was detected using a lock-in technique. For this method, the on-chip heater was mainly used, rather than those wound on to the copper blocks. If ΔT is unchanged in the field, the thermopower can be calculated by finding the zero-field value of $\tilde{S}_1$ and the thermoelectric voltage ΔV as a function of the field.

In our measurement system, we do not expect ΔT to change when the magnetic field is applied, because it is determined primarily by the thermal conductivity of the sample's sapphire substrate. We also checked the heater resistors for any magnetoresistance which could change the heat input to the system: the positive magnetoresistance measured was found to be too small to have any significant effect. There have, however, been some reports that the temperature and ΔT can change in a magnetic field[42] by as much 2% (an effect which has been attributed to magnetothermal resistances in various parts of the cryostat), while other workers[43] have found ΔT to change by less than 0.1% T^{-1}. We therefore checked to see if ΔT was affected by the field by measuring it at fields up to 1 T, and found that it was constant within the 1% measurement error. Furthermore, by measuring the magnetothermopower in both parallel and perpendicular magnetic fields, we were able to show that ΔT was constant to within 0.1% for our system for fields up to 1 T (see Sec. IV and Ref. 2). Consequently, for fields up to at least 1 T, we were able to clearly identify changes in η as small as 0.1%.

IV. RESULTS AND DISCUSSION

In this section we review the zero-field ($B=0$) behavior of the electrical conductivity and thermopower, before going on to discuss the results in both perpendicular and parallel magnetic fields.

A. Zero-field behavior

It is well known that the stress present in the (001) silicon on ($\bar{1}012$) sapphire system causes significant differences in the form of the inversion layer potential from that in an ordinary (001) Si MOS device,[44] resulting in the lowest subbands being formed from valleys in the [010] and [100] directions, with effective mass[45] around $0.42m_0$. The subbands formed from valleys in the growth direction [001] (with effective mass around $0.19m_0$) are actually higher in energy in a SOS MOSFET, whereas they form the lowest subband in an unstressed Si MOSFET. There is also a high density of dislocations, microtwins, and stacking faults in SOS due to the lattice mismatch at the Si/sapphire interface,[46] leading to the electrons in the inversion layer experiencing a highly disordered potential as compared to a Si MOSFET. The disorder and the built-in stress lead to interesting behavior in both the thermopower and the electrical conductivity.

The electrical conductivity σ as a function of electron concentration n shows an inflection close to 3.5×10^{12} cm^{-2}, which shows up as a hump in the mobility, but otherwise is what one would expect for a MOSFET (the threshold voltage is well defined at 77 K and equal to 0.5 V). This inflection in σ is characteristic of SOS MOSFET's (Ref. 44) and is due to occupation of the higher subband referred to above, with its smaller effective mass. The value of n at which it occurs is consistent with the values of stress present in the sample. There is also an anisotropy in conductivity in the [010] and [100] directions due to the stress, i.e., $\sigma_{xx}\neq\sigma_{yy}$, even at zero magnetic field (e.g., at 4.2 K and an electron concentration of 4×10^{12} cm^{-2}, $\sigma_{xx}\approx3.2\times10^{-4}$ Ω^{-1} while $\sigma_{yy}\approx2.5\times10^{-4}$ Ω^{-1}). As mentioned at the end of Sec. II A, this anisotropy does not affect any of the conclusions reached there. Note that unless otherwise stated, the current (electrical or thermal) in what follows is in the [010] direction.

As a function of temperature, the conductivity exhibited a logarithmic correction over the range studied, attributed primarily to weak localization. This allowed the method described in Sec. III B to be used for measuring temperature differences along the sample. The validity of this method was checked by measuring the thermal conductivity κ of the sapphire substrate (the ratio of the heat flux to the measuring temperature difference). We obtained a value of κ [$\mathrm{W\,m^{-1}\,K^{-1}}$]$=(0.81\pm0.01)T^3/\mathrm{K}^3$, and using the relevant phonon velocities this yielded a phonon mean free path of 920 ± 10 μm, about 10% greater than the Casimir[47] limit, implying that about 10% of the phonons were specularly reflected from the (polished) bottom surface of the substrate. This good agreement between the theoretical (Casimir) value of κ and the experimental value (especially the accurate T^3 dependence) gave us added confidence in our method of measuring the temperature difference.

The thermopower at electron concentrations of 7.0×10^{11} $\mathrm{cm^{-2}}$ and 5.9×10^{12} $\mathrm{cm^{-2}}$ is shown as a function of temperature in Fig. 3. The approximate T^3 dependence is due to the dominance of phonon-drag effects (see Sec. II C). This strong temperature dependence meant that it was not possible to see any underlying quantum corrections to the diffusion thermopower in the temperature dependence. Notice, however, that for the lower electron concentration in Fig. 3, a much better fit is obtained by including a term linear in T, i.e., the diffusion thermopower S_d. From Eq. (2.15), it is possible to extract a value for the exponent p in the energy dependence of the scattering rate, and we obtain the value $p\approx0.6$. Using this value of p to estimate S_d for the higher electron concentration gives a value of order 1 $\mu\mathrm{V\,K^{-1}}$. This shows that the theory for S_d is reasonable and that the phonon-drag thermopower really is much larger than the diffusion thermopower. As a function of electron concentration, the inverse thermopower exhibited a hump (see Fig. 4), which was attributed to occupation of the higher energy valleys,[48] as was the inflection in the conductivity which occurred at a similar electron concentration. Also from Fig. 4, it can be seen that at low n, the inverse thermopower $S^{-1}\propto n$, in accordance with theories of phonon-drag thermopower.[27] The thermopower starts to deviate from this $1/n$ dependence well before the occupation of the second subband, however, and the reason for this is not yet fully understood. It is probably related to the fact that the phonon absorption rate reaches a maximum and then slowly decreases as k_F increases.[35,49] Further details of the zero-field behavior can be found in Refs. 35 and 48. In the remainder of this paper we concern ourselves with the magnetoresistance and magnetothermopower.

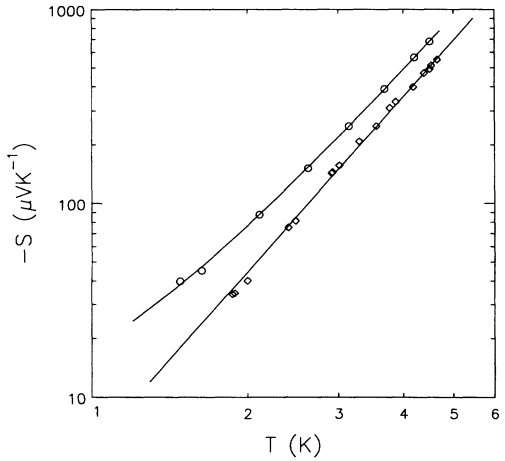

FIG. 3. Measured thermopower in SOS MOSFET for electron concentrations of 7.0×10^{11} $\mathrm{cm^{-2}}$ (circles) and 5.9×10^{12} $\mathrm{cm^{-2}}$ (diamonds). The solid lines are fits to $S=-\alpha T-\beta T^3$ for the lower electron concentration and $S=-\gamma T^3$ for the higher electron concentration, with $\alpha=10$ $\mu\mathrm{V\,K^{-2}}$, $\beta=7.0$ $\mu\mathrm{V\,K^{-4}}$, and $\gamma=5.5$ $\mu\mathrm{V\,K^{-4}}$. The T^3 dependence is a signature of phonon drag, while the linear term represents the diffusion thermopower.

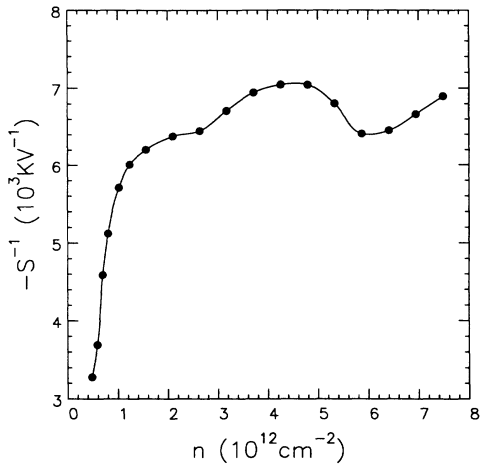

FIG. 4. Inverse of the thermopower S as a function of electron concentration at a temperature of 3.0 K. The solid line is a guide to the eye.

B. Behavior in a perpendicular magnetic field

Application of a perpendicular magnetic field resulted in a negative magnetoresistance, from which the magnetoconductivities shown in Fig. 5 were obtained. Good fits were obtained to Eq. (2.19), as shown by the solid lines, and the extracted values of $g_v\alpha$ and L_ϕ are shown in Table I, together with values of the elastic mean free path l and disorder parameter $k_F l$. The magnetoconductivity in the [100] direction showed similar behavior, but with smaller values of $g_v\alpha$. However, the ratio $\delta\sigma/\sigma$ was approximately the same for the [100] direction as for the [010] direction, in agreement with the calculations of Bhatt, Wolfle, and Ramakrishnan.[50] At the lowest temperatures studied (about 1.2 K), the magnetoconductivity started to saturate at about 1 T and eventually to decrease for fields above 2 T. This was interpreted as due to the onset of the spin-splitting (Zeeman) interaction correction (considered further in the next section). However, for the fields used in Fig. 5 (up to 0.7 T), the Zeeman interaction term is comparatively small.

TABLE I. Parameters used in fitting data in Figs. 5 and 7 to Eqs. (2.19) and (2.20), respectively: n is the electron concentration, L_ϕ is the phase relaxation length, l is an elastic scattering length, and $g_v\alpha$ is a phenomenological factor linked to intervalley scattering (see Sec. IV B). The derivatives are with respect to electron energy ε.

n (10^{12} cm^{-2})	L_ϕ (nm)	l (nm)	$g_v\alpha$	$dL_\phi/d\varepsilon$ (nm meV^{-1})	$dl/d\varepsilon$ (nm meV^{-1})	$d(g_v\alpha)/d\varepsilon$ meV^{-1}
2.10	61.5	10.1	0.55	3.8	2.0	0.11
3.18	69.0	14.3	0.74	3.4	8.6	0.04

The change in the thermopower as a function of perpendicular field is shown in Fig. 6. Since the thermopower is a composite quantity, involving the conductivity, most of the magnetothermopower is due to the suppression of the weak-localization correction to σ (see Sec. II D and Ref. 35). However, we were able to extract $\Delta\eta=\eta(B_\perp,T)-\eta(0,T)$ from the magnetothermopower and magnetoresistance data, and this is shown in Fig. 7 for two values of n. We are confident in the accuracy of our measurements from the dependence of $\Delta\eta$ on the direction of B: for a parallel field up to $\sim$0.8 T, $\Delta\eta$ is zero within the experimental uncertainty for the range of fields considered here (see Sec. IV C), in agreement with theoretical predictions.[2] The residual variation $\Delta\eta(B_\parallel)$ gives us an estimate of the relative change of ΔT with B up to 0.8 T, which turns out to be about 0.1% T^{-1}. Furthermore, the solid lines are fits to Eq. (2.20) using the parameters in Table I (assuming the phonon renormalization factor $\lambda=0$). The derivatives with respect to energy of L_ϕ, l, and $g_v\alpha$ [obtained from fits to Eq. (2.19)] were estimated by observing their variation with n; however, an anomalously large value for $dl/d\varepsilon$ had to be used to get the fit shown in Fig. 7 for the higher electron concentration data (see below). The parameter $g_v\alpha$ is really a phenomenological factor which is predicted to vary between g_v and unity as the intervalley scattering rate $1/\tau_v$ increases and becomes greater than the phase relaxation rate.[51] However, $g_v\alpha$ does not seem to follow this type of behavior; at all the electron concentrations studied it was less than unity. At the highest electron concentrations this can be explained by having a positive magnetoresistance contribution from orbital interaction processes[51] with $1/\tau_v > 1/\tau_\phi$. At the lowest electron concentration the perturbation analysis used to obtain Eq. (2.19) becomes a poor approximation (since $k_F l$ approaches 1), so that deviations of $g_v\alpha$ from theoretical values may be expected.

Since the variation of $\Delta\sigma_{xx}$ with energy becomes weaker as n increases, $\Delta\eta$ decreases as n increases so that the relative uncertainty in $\Delta\eta$ becomes larger. At the higher electron concentrations, therefore, it becomes difficult to say much that is quantitative about $\Delta\eta$. Qualitatively, however, it does become smaller with n, with values consistent with Eq. (2.20). It should be remarked here that occupation of the upper subband seems to be associated with $\Delta\eta$ reaching a maximum as a function of $B_\perp$ and then decreasing. This behavior was exhibited for all values of n above 3×10^{12} cm^{-2} but the reasons for it remain unclear.

As far as phonon renormalization is concerned, the only definitive statement that we can make is that, assum-

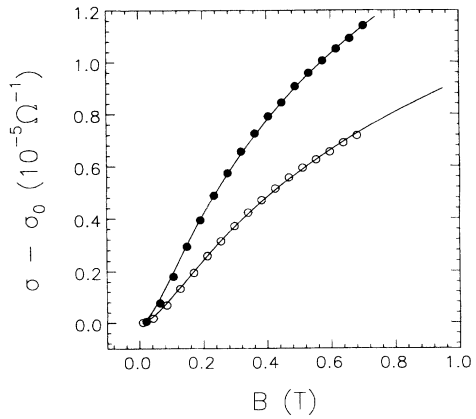

FIG. 5. The change in the conductivity as a function of perpendicular magnetic field B for electron concentrations of 2.10×10^{12} cm^{-2} (open circles) and 3.18×10^{12} cm^{-2} (filled circles). The temperature is 1.85 K. The solid lines are theoretical fits to Eq. (2.19), with the parameters shown in Table I. The zero-field values of conductivity σ_0 are 1.59×10^{-4} and 2.57×10^{-4} Ω^{-1}, respectively.

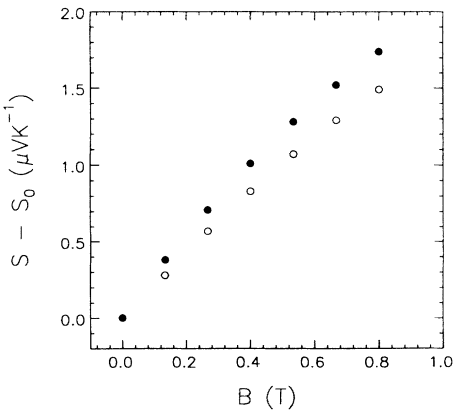

FIG. 6. The change in the thermopower as a function of perpendicular magnetic field B for electron concentrations of 2.10×10^{12} cm^{-2} (open circles) and 3.18×10^{12} cm^{-2} (filled circles). The temperature is 1.85 K. The zero-field values of thermopower S_0 are -45.0 and -39.5 μV K^{-1}, respectively.

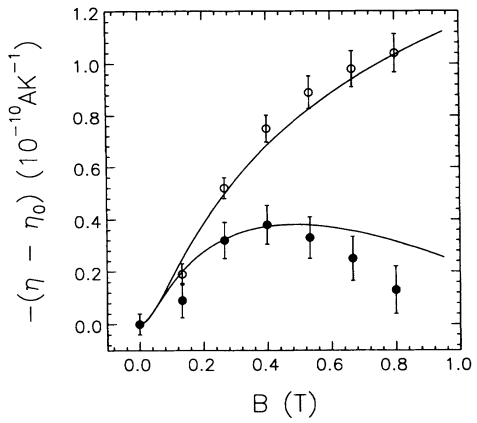

FIG. 7. The change in the thermoelectric coefficient η as a function of perpendicular magnetic field B for electron concentrations of 2.10×10^{12} cm^{-2} (open circles) and 3.18×10^{12} cm^{-2} (filled circles). The temperature is 1.85 K. The solid lines are theoretical fits to Eq. (2.20), with the parameters shown in Table I. The zero-field values η_0 are -71.6×10^{-10} and -101×10^{-10} A K^{-1}, respectively.

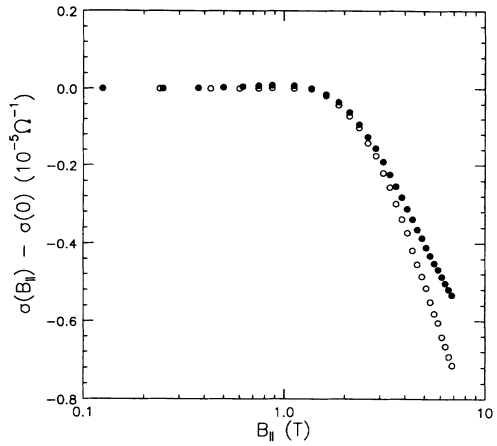

FIG. 8. The change in the conductivity as a function of parallel magnetic field $B_\parallel$ for electron concentrations of 4.26×10^{12} cm^{-2} (open circles) and 5.27×10^{12} cm^{-2} (filled circles). The temperature is 1.4 K. The zero-field values of conductivity $\sigma(0)$ are 3.22×10^{-4} and $3.82\times10^{-4}\,\Omega^{-1}$, respectively.

ing it enters Eq. (2.20) as indicated, the factor λ must be comparatively small ($\lambda \lesssim 0.1$).

C. Behavior in a parallel magnetic field

For parallel fields below about 1 T and the temperatures considered (down to about 1.5 K), both the thermopower and the resistance are constant within experimental uncertainty. Quantum interference and orbital interaction processes cannot be influenced by the field because electron trajectories in the 2D EG cannot enclose any magnetic flux. Zeeman spin-splitting effects only start to become significant when the spin-splitting energy $g\mu_B B$ is greater than the thermal energy $k_B T$. At 1.4 K, $k_B T/g\mu_B \approx 1.2$ T for $g\approx 2$. The magnetoconductivity is shown in Fig. 8 for electron concentrations of $n_1 \sim 4.3\times10^{12}$ cm^{-2} and $n_2 \sim 5.3\times10^{12}$ cm^{-2}, and it can be seen that there is no change in σ for fields below about 0.8 T. At high fields (greater than 2 T), $\Delta\sigma_{xx}(B_\parallel)$ depends approximately logarithmically on $B_\parallel$. This is in accordance with the predictions of Burdis and Dean:[52]

$$\Delta\sigma_{xx}(B) = -\frac{q^2 F^*}{4\pi^2\hbar}\mathcal{G}(b) , \tag{4.1}$$

where $b = g\mu_B B/k_B T$ and

$$\mathcal{G}(b) = 0.09b^2, \quad b \ll 1 . \tag{4.2a}$$

$$\mathcal{G}(b) = \ln[b/1.3] , \quad b \gg 1 . \tag{4.2b}$$

The renormalized screening parameter F^* can therefore be extracted[53] from the data. Similar behavior is exhibited at lower electron concentrations, although the onset of the negative magnetoconductivity is at a lower magnetic field, suggesting that there is a smaller effective g value once the upper subband becomes occupied.

For all the electron concentrations studied, the thermopower shows essentially similar behavior, as expected if the magnetothermopower is dominated by a changing σ. Again, the change from the zero-field value occurs at the same point for a given electron concentration, but this point varies with n, implying a change in g.

For the low values of magnetic field used when the field was perpendicular to the 2D EG, we showed above that ΔT varied very little with B and so we could extract $\Delta\eta = \eta(B) - \eta(0)$. However, at the higher fields used here, we can only say that $\Delta T(B)$ is constant to within the accuracy to which we can directly measure it, in this case about 1%. Thus we define a quantity ξ by

$$\xi(B) = \frac{\sigma_{xx}(B)\Delta V_1(B)}{\Delta T(0)} - \eta(0) , \tag{4.3}$$

which contains only quantities which we can measure relatively easily. It is easy to show that ξ can also be written as

$$\xi(B) = \frac{\Delta T(B)}{\Delta T(0)}\eta(B) - \eta(0) , \tag{4.4}$$

so that $\xi(B) = \Delta\eta(B)$ if ΔT does not change with field; otherwise

$$\xi(B) = \eta(0)\left[\frac{\Delta T(B)}{\Delta T(0)} - 1\right] + \frac{\Delta T(B)}{\Delta T(0)}\Delta\eta(B) . \tag{4.5}$$

This quantity ξ is shown in Fig. 9 for the same electron concentrations as Fig. 8. It is tempting to conclude that the resulting variation in ξ is due solely to interaction effects, but the possibility of a change in $\Delta T(B)$ must be allowed for. From direct measurements we found that $\Delta T(B)$ changed by only 1% for fields up to 7 T, with a 1% measurement uncertainty (i.e., ΔT was constant within the experimental accuracy). This then enables us to put some bounds on $\Delta\eta(B_\parallel)$ using Eq. (4.5).

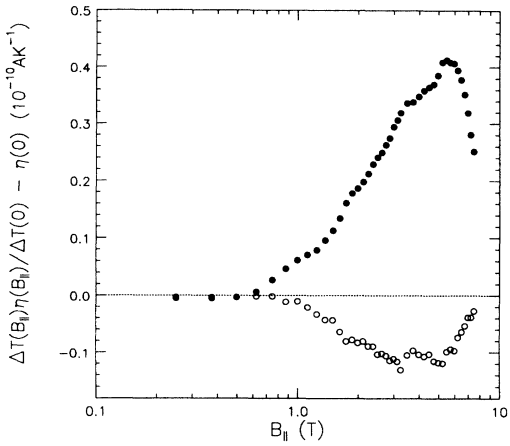

FIG. 9. The change in the parameter $\xi=[\Delta T(B_\parallel)\eta(B_\parallel)/\Delta T(0)-\eta(0)]$ as a function of parallel magnetic field $B_\parallel$ for electron concentrations of 4.26×10^{12} cm^{-2} (open circles) and 5.27×10^{12} cm^{-2} (filled circles). The temperature is 1.4 K. The zero-field values $\eta(0)$ are -53.1×10^{-10} and -66.3×10^{-10} A K^{-1}, respectively.

For the higher electron concentration n_2, we know that $\eta(0)\approx-66\times10^{-10}$ A K^{-1} and that $\xi=(4.0\pm0.1)\times10^{-11}$ A K^{-1} at a field of about 6 T with a change in ΔT of less than about 2%, so that Eq. (4.5) gives

$$(4.0\pm0.1)\times10^{-11}=-66\times10^{-10}\times(\pm0.02)+(1\pm0.02)\Delta\eta. \tag{4.6}$$

This means immediately that $|\Delta\eta|<2\times10^{-10}$ A K^{-1}, or as a relative change, $|\Delta\eta/\eta|<3\%$. We may obtain a lower bound by remembering that if all of the variation in ξ were entirely due to variations in ΔT, then ξ would show a similar trend with magnetic field, independent of the electron concentration: in particular *it would always be of the same sign.* The fact that ξ can be of either sign suggests that it is reflecting an underlying change in η with field, together with the (possible) changes in ΔT. Noting that the orbital effects are zero here (since the field is parallel to the 2D EG), we suggest that the underlying change in η arises from electron-electron interaction effects, and that it is very sensitive to the occupation of the upper subband, possibly changing sign.

As an example, consider the values of ξ at 6 T again. If we were to assume that all of $\xi(n_1)$ was due to a change in ΔT with field [i.e., $\Delta\eta(n_1)\equiv0$], then Eq. (4.5) would give $[\Delta T(B)/\Delta T(0)-1]\approx0.002$. Since we do not expect ΔT to depend upon the electron concentration, we can put this value for $[\Delta T(B)/\Delta T(0)-1]$ into Eq. (4.5) to obtain $\Delta\eta(n_2)\approx5.3\times10^{-11}$ A K^{-1}. Similarly, if we assumed all of $\xi(n_2)$ was due to a change in ΔT with field, we would obtain $[\Delta T(B)/\Delta T(0)-1]\approx-0.006$ and $\Delta\eta(n_1)\approx-4.1\times10^{-11}$ A K^{-1}. Our experimental results therefore demonstrate that even if $\Delta\eta$ was zero at one of n_1,n_2, it would be nonzero at the other. Furthermore, by calculating $|\Delta\eta(n_1)|$ and $|\Delta\eta(n_2)|$ from the experimental data for various values of $[\Delta T(B)/\Delta T(0)-1]$, it can be demonstrated that at least one of them is greater than about 2.5×10^{-11} A K^{-1}. Thus we can say that at about 6 T, in a silicon-on-sapphire inversion layer, the following inequality will hold for at least one of the electron concentrations n_1 and n_2: $2.5<|\Delta\eta/10^{-11}\,\text{A K}^{-1}|<20$. Thus it is fairly clear that $|\Delta\eta(B_\parallel)|\neq0$, even though we can say little about its sign. Referring back to Fig. 8, we find that $|\Delta\sigma_{xx}/\sigma_{xx}|\approx1.3\%$ at a similar magnetic field, so that σ and η are affected to the same order of magnitude by the magnetic field. Similar conclusions can be reached by considering the lower electron concentrations.

V. CONCLUSIONS

We have discussed aspects of thermoelectric transport in disordered two-dimensional systems and presented some experimental measurements of the effects of quantum interference and electron-electron interactions upon the thermoelectric transport parameter η, using silicon-on-sapphire MOSFET's. Phonon-drag effects give η a strong temperature dependence which masks the quantum interference and interaction effects as a function of T, so we investigated them by applying magnetic fields both perpendicular ($B_\perp$) and parallel ($B_\parallel$) to the 2D EG. Quantum interference led to a small change in η with $B_\perp$, which was in accordance with theory and qualitatively different to the change in σ.

In a parallel magnetic field, we found that η also changed but we could only put upper and lower limits on the magnitude of this change. However, our experiments do seem to indicate that $\Delta\eta$ is nonzero for a magnetic field parallel to the 2D EG. We suggest this nonzero $\Delta\eta$ arises from electron-electron interaction effects.

Further experiments in which the temperature gradient is determined more accurately will help in finding out the form of the changes in η in more detail, while calculations concerning the effect of a parallel magnetic field upon η would be useful in deciding whether the nonzero $\Delta\eta(B_\parallel)$ is indeed due to electron-electron interactions. The role of phonon drag and phonon renormalization in influencing the magnetic-field dependences could also be clarified further, but we do not expect this to significantly alter any of our conclusions.

ACKNOWLEDGMENTS

We would like to thank M. Pepper for many useful discussions and B. L. Gallagher for guidance with some of the experimental measurements. We are grateful to A. Gundlach at the University of Edinburgh Microfabrication Facility for making the SOS MOSFET's used in this work.

[1]See, e.g., P. A. Lee and T. V. Ramakrishnan, Rev. Mod. Phys. **57**, 287 (1985).
[2]M. J. Kearney, R. T. Syme, and M. Pepper, Phys. Rev. Lett. **66**, 1622 (1991).
[3]For an introduction to phonon renormalization, see M. A. Howson and B. L. Gallagher, Phys. Rep. **170**, 265 (1988).
[4]Yu. G. Gurevich and O. L. Mashkevich, Phys. Rep. **181**, 327 (1989).
[5]See, e.g., G. D. Mahan, *Many Particle Physics* (Plenum, New York, 1981).
[6]G. V. Chester and A. Thellung, Proc. Phys. Soc. **77**, 1005 (1961).
[7]M. J. Kearney and P. N. Butcher, J. Phys. C **21**, L265 (1988).
[8]See also L. Smrcka and P. Streda, J. Phys. C **10**, 2153 (1977).
[9]A very elegant demonstration of this has been provided recently by V. Bayot, L. Piraux, J. P. Michenaud, and J. P. Issi, Phys. Rev. Lett. **65**, 2579 (1990).
[10]B. L. Gallagher, J. P. Oxley, T. Galloway, M. J. Smith, and P. N. Butcher, J. Phys. Condens. Matter **2**, 755 (1990) and references therein.
[11]G. Strinati and C. Castellani, Phys. Rev. B **36**, 2270 (1987).
[12]C. S. Ting, A. Houghton, and J. R. Senna, Phys. Rev. B **25**, 1439 (1982).
[13]V. V. Afonin, Yu. M. Gal'perin, and V. L. Gurevich, Zh. Eksp. Teor. Fiz. **87**, 335 (1984) [Sov. Phys. JETP **60**, 194 (1984)]; V. V. Afonin, Yu. M. Gal'perin, and V. L. Gurevich, Phys. Rev. B **33**, 8841 (1986); C. Castellani, C. Di Castro, M. Grilli, and G. Strinati, *ibid.* **37**, 6663 (1988).
[14]See M. J. Burns and P. M. Chaikin, Phys. Rev. B **27**, 5924 (1983).
[15]J. W. P. Hsu, A. Kapitulnik, and M. Yu. Reizer, Phys. Rev. B **40**, 7513 (1989).
[16]M. Fabrizio, C. Castellani, and G. Strinati, Phys. Rev. B **43**, 11 088 (1991).
[17]A. Schmid, Z. Phys. **259**, 421 (1973).
[18]M. Yu. Reizer and A. V. Sergeev, Zh. Eksp. Teor. Fiz. **90**, 1056 (1986) [Sov. Phys. JETP **63**, 616 (1986)].
[19]B. L. Al'tshuler, Zh. Eksp. Teor. Fiz. **75**, 1330 (1978) [Sov. Phys. JETP **48**, 670 (1978)].
[20]M. Yu. Reizer and A. V. Sergeev, Zh. Eksp. Teor. Fiz. **92**, 2291 (1987) [Sov. Phys. JETP **65**, 1291 (1987)].
[21]S. K. Lyo, Phys. Rev. B **17**, 2545 (1978); A. Vilenkin and P. L. Taylor, *ibid.* **18**, 5280 (1978); A. B. Kaiser, *ibid.* **29**, 7088 (1984), and references therein.
[22]M. Yu. Reizer and A. V. Sergeev, Zh. Eksp. Teor. Fiz. **93**, 2191 (1987) [Sov. Phys. JETP **66**, 1250 (1987)].
[23]J. L. Opsal, B. J. Thaler, and J. Bass, Phys. Rev. Lett. **36**, 1211 (1976).
[24]M. Jonson and G. D. Mahan, Phys. Rev. B **42**, 9350 (1990).
[25]See, e.g., R. D. Barnard, *Thermoelectricity in Metals and Alloys* (Taylor and Francis, London, 1972).
[26]D. G. Cantrell and P. N. Butcher, J. Phys. C **20**, 1985 (1987).
[27]M. J. Smith and P. N. Butcher, J. Phys. Condens. Matter **2**, 2375 (1990), and references therein.
[28]S. M. Girvin and M. Jonson, J. Phys. C **15**, L1147 (1982).
[29]M. Jonson and S. M. Girvin, Phys. Rev. B **29**, 1939 (1984).
[30]See, e.g., R. Fletcher, J. C. Maan, K. Ploog, and G. Weimann, Phys. Rev. B **33**, 7122 (1986); B. L. Gallagher, J. P. Oxley, T. Galloway, M. J. Smith, and P. N. Butcher, J. Phys. Condens. Matter **2**, 755 (1990), and references therein.
[31]S. R. de Groot and P. Mazur, *Non-equilibrium Thermodynamics* (Dover, New York, 1984).
[32]For some recent work on nonlinear thermoelectric transport see A. N. Grigorenko, P. I. Nitkin, D. A. Jelski, and T. F. George, Phys. Rev. B **42**, 7405 (1990), and references therein.
[33]G. D. Mahan, Phys. Rev. B **43**, 3945 (1991).
[34]R. T. Syme, M. J. Kelly, and M. Pepper, J. Phys. Condens. Matter **1**, 3375 (1989).
[35]Further details of this and the experimental methods can be found in R. T. Syme, Ph.D. thesis, University of Cambridge, United Kingdom, 1989 (unpublished).
[36]N. V. Zavaritskii, Physica **126B**, 369 (1984); G. M. Gusev, N. V. Zavaritskii, Z. D. Kvon, and A. A. Yurgens, Pis'ma Zh. Eksp. Teor. Fiz. **40**, 275 (1984) [JETP Lett. **40**, 1056 (1984)].
[37]H. Obloh, K. von Klitzing, and K. Ploog, Surf. Sci. **142**, 236 (1984).
[38]R. Fletcher, M. D'Iorio, W. T. Moore, and R. Stoner, J. Phys. C **21**, 2681 (1988).
[39]R. Fletcher, M. D'Iorio, A. S. Sachrajda, R. Stoner, C. T. Foxon, and J. J. Harris, Phys. Rev. B **37**, 3137 (1988).
[40]J. S. Davidson, E. D. Dahlberg, A. J. Valois, and G. Y. Robinson, Phys. Rev. B **33**, 2941 (1986).
[41]B. L. Gallagher, C. J. Gibbings, M. Pepper, and D. G. Cantrell, *Proceedings of 18th International Conference on The Physics of Semiconductors* (World Scientific, Singapore, 1987), p. 1539.
[42]R. Fletcher, J. J. Harris, and C. T. Foxon, Semicond. Sci. Technol. **6**, 54 (1991).
[43]J. P. Eisenstein, A. C. Gossard, and V. Narayanamurti, Phys. Rev. Lett. **59**, 1341 (1987).
[44]S. Kawaji, K. Hatanaka, K. Nakamura, and S. Onga, J. Phys. Soc. Jpn. **41**, 1073 (1976).
[45]T. Englert, G. Landwehr, J. Pontcharra, and G. Dorda, Surf. Sci. **98**, 427 (1980).
[46]S. Cristoloveanu, Rep. Prog. Phys. **50**, 327 (1987).
[47]H. B. G. Casimir, Physica **5**, 495 (1938).
[48]R. T. Syme, M. Pepper, A. Gundlach, and A. Ruthven, Superlatt. Microstruct. **5**, 103 (1989).
[49]J. C. Hensel, B. I. Halperin, and R. C. Dynes, Phys. Rev. Lett. **51**, 2302 (1983).
[50]R. N. Bhatt, P. Wolfle, and T. V. Ramakrishnan, Phys. Rev. B **32**, 569 (1985).
[51]H. Fukuyama, in *Electron-Electron Interactions in Disordered Systems,* edited by A. L. Efros and M. Pollak (North-Holland, Amsterdam, 1985).
[52]M. S. Burdis and C. C. Dean, Phys. Rev. B **38**, 3269 (1988).
[53]R. T. Syme and M. Pepper, J. Phys. Condens. Matter **1**, 2747 (1989).

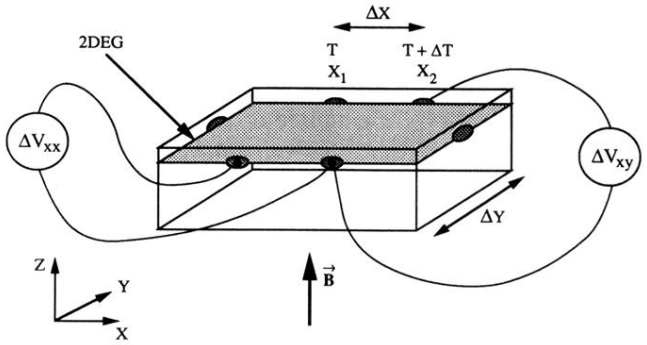

FIG. 1. Schematic diagram of our sample, showing directions of **B** and ∇T.

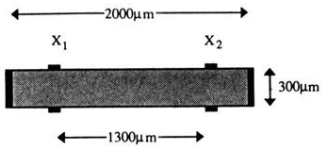

(a)

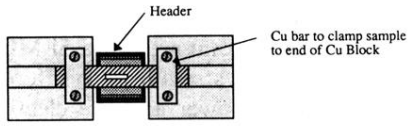

(b)

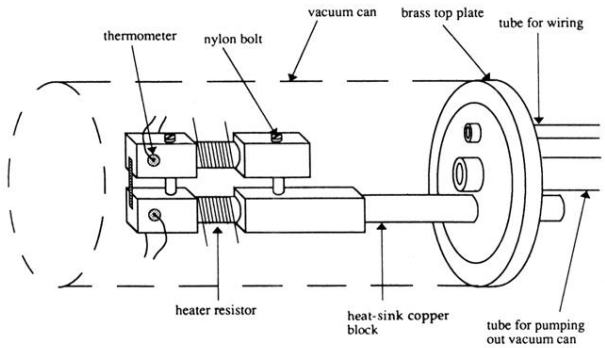

(c)

FIG. 2. (a) Geometry of MOSFET's used in this work. (b) Arrangement for clamping sample to end of insert. (c) Diagram of the insert used to measure the thermopower.